

Elijah Boardman<sup>1</sup>; Boardman, Joseph;<sup>2</sup> Dethier, Evan<sup>1</sup>; McGurk, Bruce<sup>3</sup>; Renshaw, Carl<sup>1</sup>  
<sup>1</sup>*Dartmouth College Earth Sciences Department*; <sup>2</sup>*Analytical Imaging and Geophysics, LLC*;  
<sup>3</sup>*McGurk Hydrologic*

**Calibration of a High-Discharge Wilderness Rating Curve Using Distributed SWE Maps:  
Water Balance Considerations for the Tuolumne River Headwaters**

*DRAFT COPY*

2021

*DRAFT COPY*

**Abstract**

Constructing a relative time-dependent water balance for the headwaters subbasin of the Hetch Hetchy Reservoir drainage area reveals a discrepancy between the distribution of snow water equivalent (SWE) and reported stream discharge. Due to the location of the headwaters gage in the Yosemite Wilderness, the gage's current rating curve was generated through hydraulic analysis of survey-derived cross-sections instead of traditional trolley-based direct discharge measurements. Past studies have postulated that differential precipitation distribution could explain the relatively low runoff from the headwaters basin compared to reservoir inflows accumulating from the full basin. However, we use high spatial resolution maps of SWE measured over 7 yearly campaigns by the NASA/JPL Airborne Snow Observatory (ASO) to determine that snow loading in the headwaters subbasin is approximately proportional to its total area, suggesting that differential precipitation does not account for the relative water balance discrepancy. Hence, we encounter a problem of water mass conservation, suggesting that the gage underreports net discharge. We identify periods of roughly equal snowmelt and reservoir inflow to reconstruct proxy high-stage discharge values during portions of the 2013–2019 melt seasons. We combine the SWE proxies with the original stage record and low-stage field measurements from the U.S. Geological Survey (USGS) to optimize a new power-law rating curve which reduces the mean melt-season error in our relative mass-balance model to 6%, as compared to 40% error using current discharge values over the same timeframe. Thus, we demonstrate a new method for calibrating high-stage flows at the Tuolumne headwaters gage by comparing distributed SWE maps with known reservoir inflows. Validation of the recalibrated rating curve also reveals the importance of temperature-isotherm hypsometry for driving the seasonal dependence of relative subbasin water balances.

## Introduction

The upper Tuolumne River is the main tributary to Hetch Hetchy Reservoir, the first in a series of reservoirs which deliver municipal water and hydroelectric power to San Francisco. From its headwaters on the high alpine peaks of Yosemite National Park, the river courses through alpine meadows, montane forests, and bedrock canyons before encountering O'Shaughnessy Dam, which impounds Hetch Hetchy Reservoir. The upslope area of the Reservoir is 1178 sq. km., broadly divisible into two regions: a headwaters subbasin consisting of 66% of the total area (780 sq. km.) which drains through the Tuolumne Grand Canyon Gage (USGS #11274790), and a set of side basins which drain mostly unged into the reservoir.

To establish the Reservoir water budget, McGurk Hydrologic calculates unimpeded natural inflows to Hetch Hetchy through consideration of smoothed Reservoir water level, power station draft, and downstream discharge from dam releases (McGurk 2021). Managers at the Hetch Hetchy Reservoir in California's Sierra Nevada mountain range have historically considered stream gages and localized snow-monitoring techniques to determine the relative contribution of different tributaries to the Reservoir's water supply. While the lower stream gage below O'Shaughnessy Dam is considered highly reliable due to the morphology of the gaged reach and the long-established set of measurements (McGurk 2021, personal communication), the headwaters stem of the Tuolumne River flows through the highly protected Yosemite Wilderness, so traditional rating-calibration techniques used on high-discharge rivers (such as trolley installations) are not permitted. When the USGS installed the gage in 2006, the agency surveyed a series of channel cross-sections and used critical flow analysis to derive a rating curve. The USGS has also performed a series of direct discharge measurements at low stage from 2006 to 2020, including minor shift-adjustments (USGS 2021). The highest directly measured stream flow is 538 cfs, an order of magnitude lower than peak flows at this site.

In 2013, the NASA/JPL Airborne Snow Observatory (ASO) project began overflights of the Tuolumne region with scanning lidar and an imaging spectrometer to map spatially distributed snow depth and albedo which they combine with density fields from the iSnobal snowmelt model to generate a timeseries of high-resolution SWE maps for the region (Painter et al., 2016). The direct incorporation of ASO data into the existing iSnobal melt model increased the correlation of modeled and measured snow depth values from an  $r^2$  of 0.162 to an  $r^2$  of 0.899 according to an analysis by Hedrick et al. (2018), showing the efficacy of this new approach to

snowpack quantification. In these highly snow-dominated basins, a ratio of ASO-measured SWE to runoff thus provides insight into the overall catchment water balance.

It is desirable to establish the relative contribution of different subbasins to the annual Hetch Hetchy Reservoir water supply in order to better predict and manage yearly runoff. Comparison of water balances in the headwaters subbasin and the full basin indicate a discrepancy in relative snow and runoff ratios.

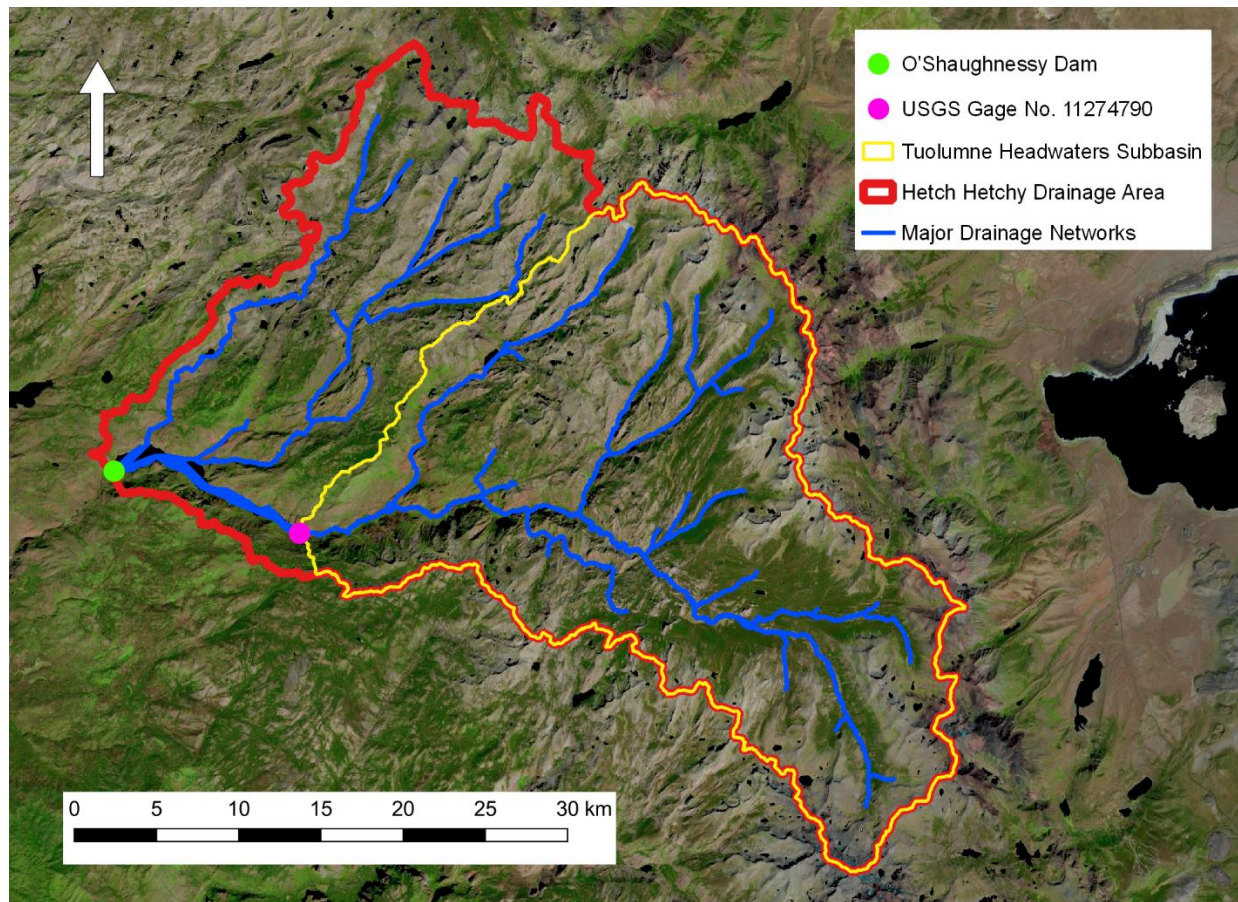


**Figure 1: Map of the Hetch Hetchy Reservoir watershed**

*The O'Shaughnessy Dam (green dot) impounds Hetch Hetchy Reservoir on the main fork of the Tuolumne River in California's Sierra Nevada. The catchment area for Hetch Hetchy (red polygon) includes a headwaters subbasin (yellow polygon) which drains through USGS Gage Number 11274790 "TUOLUMNE R A GRAND CYN OF TUOLUMNE AB HETCH HETCHY" (pink dot). Blue lines indicate major stream networks. The headwaters subbasin includes 66% of the Reservoir's total upslope area. Terrain varies from alpine peaks (extending to about 4000 m) to low montane forests (dropping to about 1100 m at the Reservoir).*

First, we compare the relative partitioning of snow into the headwaters region by spatially summing ASO SWE maps (Painter et al. 2019) within the full basin and subbasin catchments. The headwaters subbasin contains a mean of 69% of the total SWE in the Hetch Hetchy drainage basin throughout the snow-dominated months of January to July, trending to slightly higher relative SWE content later in the melt season, primarily due to highly concentrated regions of lingering snow in high alpine cirques. The headwaters subbasin has 66% of the area of the full basin, indicating slightly above-average SWE content in the overall headwaters region.

Second, we compare integrated USGS-reported headwaters discharge and unimpeded Hetch Hetchy Reservoir inflow on periods between ASO mapping flights since these flights provide temporal bounds on the observation periods. The headwaters gage reports discharge levels only amounting to a mean of 42% of the total reservoir inflow across these intervals. The current stream gage implies that the headwaters subbasin underperforms the whole basin in net discharge despite the SWE maps showing above average snow loading.

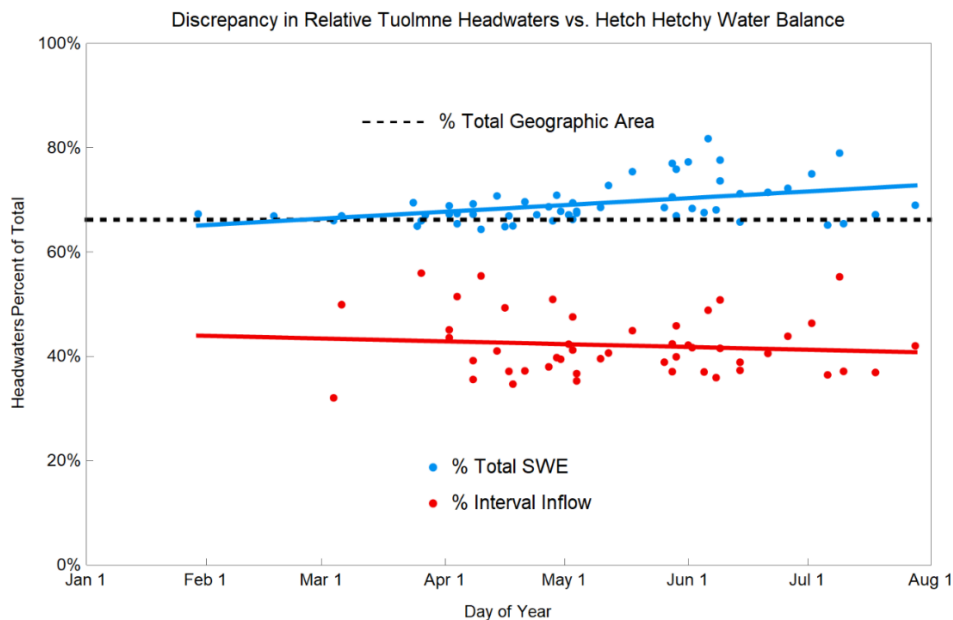


**Figure 2: Discrepancy in relative balances of SWE and runoff for the headwaters subbasin**

*The proportion of total full basin SWE located in the headwaters subbasin is plotted in blue, showing that the headwaters snow loading is approximately proportional to its geographic area (dashed line) in the early season and slightly increases later. The proportion of reservoir inflow reported by the headwaters gage during inter-flight SWE measurement intervals is plotted in red, showing a much lower mean and opposite trend compared to the relative snow distribution. We interpret this as a water balance discrepancy.*

## Methods

To explore the discrepancy between relative SWE content and runoff generation in the headwater subbasin, we examine the seasonal snowmelt water balance for the headwaters gage by comparing cumulative reservoir inflows to cumulative snowmelt and discharge through the headwaters gage from the first ASO flight of each year through July 31. Across water years 2013–2019, we calculate net SWE changes across the full basin and headwaters subbasins on each inter-flight measurement interval since SWE is constrained within these intervals. We sum all negative changes (net SWE loss periods) to approximate total measured spring snowmelt. We zero-out intervals with increasing snowpack periods in order to capture the time-dependent rebuilding of the snowpack, because in some years, the sum of losses can be substantially larger than the total snowpack at any one time: in 2015, the sum of SWE losses through June 8 was 40% more than the maximum instantaneously measured SWE amount on March 5. Ongoing research by Boardman et al. (2021, unpublished) supports the assumption that sublimation is negligible in the melt period, thus suggesting that SWE loss measured in this way is a good approximation for net SWE melt.

To normalize between years, we calculate a full-basin yearly offset value by differencing the sum of SWE losses with the cumulative Hetch Hetchy inflow from the first flight date through the end of July. The yearly offset compensates for yearly variables such as precipitation in non-snow-covered areas, evapotranspiration, and storage changes. We assume negligible impact of elevation- and location-dependence in physical variables affecting runoff such as lithology, morphology, and landcover; in general we assume that the headwaters subbasin functions similarly to the full catchment on seasonal timescales, and this assumption is supported by additional ongoing modeling research in the Tuolumne by Boardman et al. (2021, unpublished). Thus, we scale the yearly offset linearly with area and add it to the summed SWE melt to estimate cumulative runoff from the first flight date through July 31.

$$\text{Yearly Offset Through July 31} = \left[ \int_{\text{First Flight}}^{\text{July 31}} \text{Inflow} * dt - \left( \sum_{\substack{\text{Net-Loss} \\ \text{Flight Intervals}}} \text{SWE Melt} \right) \right] \frac{\text{Area}}{\text{Full Basin Area}}$$

### Equation 1: Calculation of the yearly offset of full-basin inflows vs. measured SWE melt

*The offset allows for normalization between years by assuming an area-dependent difference between measured SWE loss and full-basin inflow.*

Rearranging terms in the offset equation allows us to solve for expected seasonal discharge, resulting in our water balance input model. The yearly offset accounts for the seasonal variation in runoff ratio as well as snowpack rebuilding and liquid precipitation, all of which are effects demonstrated in Boardman et al. (2021 unpublished).

$$Input\ Model = \left( \sum_{\substack{Net-Loss \\ Flight\ Intervals}} SWE\ Melt \right) + \left( \begin{matrix} Yearly\ Offset \\ Through\ July\ 31 \end{matrix} \right)$$

**Equation 2: Input model for the Tuolumne water balance**

*The input model calculates the amount of expected water arriving at the gage or flowing into the reservoir across a given time period. We sum SWE melt across net-loss inter-flight periods and add an area-scaled offset (Equation 1) to account for other hydrological unknowns.*

Our output model consists of integrated runoff from the day after the year’s first ASO flight date through July 31. We start integrating runoff on the day after a given flight because the measured SWE cannot instantly enter the stream, and we choose July 31 as the end point because ASO flights show that most snowmelt occurs by mid-July and this period additionally brackets the highest flows of each year. For the full Hetch Hetchy drainage area, we obtain integrated runoff from the daily calculated unimpeded inflow values (McGurk 2021), but for the headwaters gage, it is necessary to apply a rating curve to convert stage data to runoff. The existing published discharge measurements include small shift-adjustments, and we use these values for evaluating the existing model. To create our new model, we disregard the slight shift adjustments and apply our new rating curve to the stage record across the ASO record period.

$$Output\ Model = \int_{\substack{July\ 31 \\ First\ Flight}} Q * dt$$

**Equation 3: Output model for the Tuolumne water balance**

*The output model integrates discharge (Q) reported by the gage or observed reservoir inflow across a given time period.*

Ratioing the difference of input and output models over the input yields a yearly estimate of relative water balance error, or the percentage of the melt-season water balance which remains unaccounted. The water balance error can be positive or negative depending on the year and the chosen rating curve; although the ideal is zero water balance error at all times, we desire minimally acceptable results to at least show no systematic bias with regard to over- or under-prediction across seasonal or multi-year timeframes.

$$\text{Relative Water Balance Error} = \frac{\text{Output Model} - \text{Input Model}}{\text{Input Model}}$$

#### **Equation 4: Relative water balance model**

*We calculate relative water balance error at two flux gates: the headwaters gage and the reservoir boundary. In each case, the difference of expected water (Input Model) and observed water (Output Model), normalized by the expected magnitude, gives the percent error resulting from the water's passage through the flux gate. Since our flux gates are one-dimensional (line across the creek or reservoir boundary), we expect zero real effect as the water passes through, and non-zero water balance error represents error in either the Input or Output Models or both.*

Applying the water balance error model to the full basin yields 0% error by definition, since we calculate the yearly offsets using the inverse of the same model. However, using the USGS 15-minute discharge record (interpolated across missing points) to calculate relative water balance error for the headwaters subbasin results in consistent underestimation of discharge, averaging -40% relative water balance error across the melt season of 2013–2019, with no value better than -35% water balance error (in 2015). As such, the survey-derived model does not produce acceptable results because all errors are systematically biased to underreporting runoff.

Thus, we attempt to close the water balance by recalibrating the headwaters rating curve using interval values of SWE loss as a proxy for high-stage discharge measurements. We calculate the interval runoff ratio between net SWE change and integrated reservoir inflows on all periods between ASO mapping flights, including the day of the final flight but not the initial flight in the temporal integration period, thereby assuming that variations in travel time are negligible on the timescales involved herein. In a sample daily hydrograph for the gage in April 2021, we observe a clear diurnal peak flow occurring around midnight, supporting the assumption of sub-12-hour travel time for meltwater in this catchment (USGS 2021).

$$\text{Interval Runoff Ratio Between Flights } A, B = \frac{SWE_{\text{Flight } B} - SWE_{\text{Flight } A}}{\int_{\text{Flight } A \text{ Date} + 1 \text{ Day}}^{\text{Flight } B \text{ Date}} \text{Reservoir Inflow} * dt}$$

### **Equation 5: Snowmelt interval runoff ratio**

*The runoff ratio gives the ratio of SWE loss to integrated runoff. On periods where all other variables are negligible or offsetting, the runoff ratio will be 1.*

The complex nature of large alpine basins results in a varying relationship between SWE loss and integrated runoff on any single inter-flight measurement period (Boardman et al. 2021, unpublished). However, the ability to fix both sides of the full-basin water balance using SWE change and reservoir inflows enables the selection of 18 measurement periods with full-basin interval runoff ratios of approximately 100% ( $\pm 20\%$ ), with at least one acceptable period selected from each of the 2013–2019 melt seasons. We assume that the subbasin behaved similarly to the full basin during these 18 intervals, thus positing a rough 1:1 relationship between headwaters SWE loss and integrated headwaters discharge during the selected periods.

We obtain the USGS 15-minute stage record across the water years of 2013–2020 (USGS 2021) to calculate discharge based on the modeled rating curve. Some stage data points are missing from the record, including a few full days, and we linearly interpolate between known stages in these cases. We model net interval runoff by summing the 15-minute discharge contributions calculated using the power-law rating equation (Rantz, 1982).

$$Q = P(G - e)^N$$

$N, P \rightarrow \text{constants}; e \equiv G_{Q=0}$

### **Equation 6: Power-law rating equation (Rantz, 1982)**

*The power-law rating equation gives discharge,  $Q$ , as a function of gage height,  $G$ , dependent on the zero-discharge stage offset,  $e$ , and two unknown constants,  $N$  and  $P$ .*

We use a minimum-stage value of  $e = 5.75$  copied from the highest stage at which the USGS-surveyed rating curve, published as tabulated ( $G, Q$ ) value pairs, indicates zero discharge. We create a combined optimization function using the relative water balance error equation with offsets of zero (implied 100% interval runoff ratio) forced with both the 18 selected ASO SWE loss measurements and the 39 low-stage field measurements from the USGS.

$$\text{Water Balance Error} = \sum_{\text{SWE Loss Periods}} \left| \frac{\int Q_{\text{Modeled}} - \text{SWE Loss}}{\text{SWE Loss}} \right| + \sum_{\text{Field Measurements}} \left| \frac{Q_{\text{Modeled}} - Q_{\text{Measured}}}{Q_{\text{Measured}}} \right|$$

**Equation 7: Optimization function for total low- and high-stage water balance error**

*The total water balance optimization function includes the relative water balance error at low stage (based on USGS observations) and high stage (based on the SWE-discharge proxies). The linear nature of the model is resistant to outliers (as opposed to a least-squares approach).*

We use simulated annealing numerical optimization due to its resilience in escaping local minima (Wolfram Research, 2020) to minimize the water balance error simultaneously at low and high stages by optimizing the paired values of (*N*, *P*) in the power-law rating equation.

**Results**

The water balance error is minimized with the value pair *N* = 2.7501, *P* = 10.2544. Inserting these values into Eq. 5 results in a new rating curve which closely matches the USGS survey-derived rating curve at low stages (*G* < 8 ft.) but predicts more than twice as much discharge at high stages (*G* > 14 ft.). To test the goodness of fit for this model, we repeat the calculation of relative water balance error (Eq. 3) using the 15-minute stage record from the day after the first ASO flight through July 31 of the years 2013–2019 in the same fashion as the initial evaluation of rating curve error. The mean absolute value of the seasonal error using the proposed new rating curve is 6%, with extrema of -10% (2015) and +15% (2019).

Year	Discrepancy: Original USGS	Discrepancy: Remodeled
2013	-39%	-1%
2014	-36%	-1%
2015	-35%	-10%
2016	-43%	2%
2017	-48%	7%
2018	-38%	9%
2019	-43%	15%

**Table 1: Percentage of cumulative melt-season water balance error by year**

*The surveyed rating curve always underpredicts seasonal discharge on the study period, but the new SWE-derived rating curve reduces both the overall error and the bias.*

We analyze the stability of the numerical model by performing jackknife resampling with the set of 18 SWE melt discharge proxies by repeating the optimization with all but one of the SWE measurement periods. (We use all 39 low-stage USGS measurements in all cases.) The results indicate a stable model: all modeled rating curves are within  $\pm 1\%$  of each other across the range of observed stages. Further, repeating the calculation for the relative water balance error, as above, results in mean values within 0.1% of the full model's mean yearly error. Thus, we demonstrate that the model is stable with respect to the SWE loss forcing data, suggesting the validity of treating SWE loss as a proxy for discharge across the 18 selected measurement periods and supporting the accuracy of the new rating curve.

$N =$	2.xxx	747	749	750	746	751	749	750	747	751	751	749	753	749	753	751	751	750	754
$P =$	10.xxx	284	244	256	351	235	242	266	333	235	243	246	226	246	224	237	236	241	223

**Table 2: Optimized values of  $(N, P)$  under jackknife resampling of SWE-discharge proxies**

*Values are listed as thousandths, i.e. the first set is  $(N = 2.747, P = 10.284)$ , etc. Jackknife resampling of the 18 SWE melt intervals shows that the optimization model is mathematically stable, since all of the resampled rating curves are within 1% of each other over the full window of observed stages.*

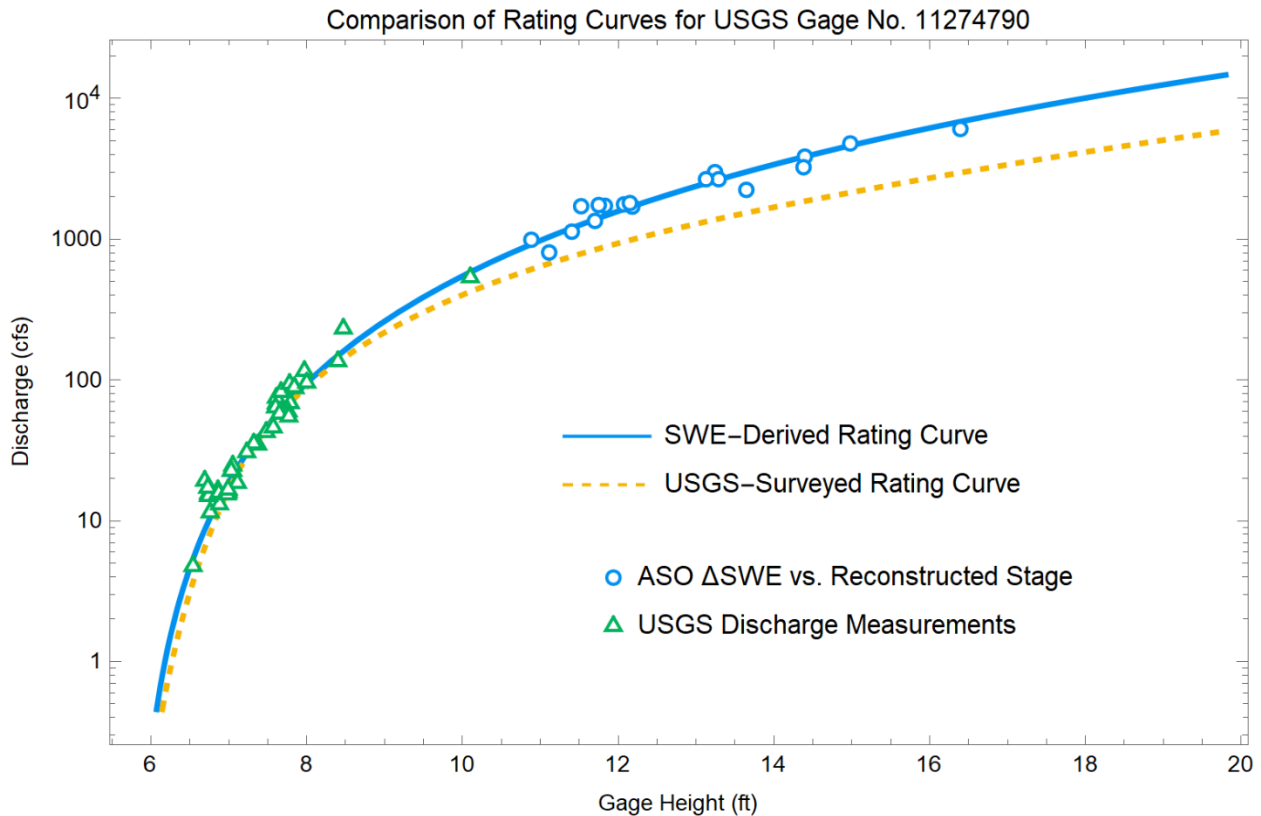


**Figure 3: Comparison of SWE-derived\* and USGS-surveyed rating curves**

*The green points represent USGS field discharge measurements and corresponding stage, and the blue points represent ASO SWE-loss measurements between selected flight intervals plotted against implied constant stages reconstructed as roots of the rating curve for the modeled net discharge (not to be confused with the actual average stages, since the stage-discharge relationship is nonlinear). We use the SWE changes and the USGS low-stage discharge data to fit a power law to these data, creating a new rating curve. The USGS-surveyed rating curve is plotted in yellow, with the proposed new rating curve plotted in blue. Both rating curves are similar in the low-flow regime, but deviate substantially at high stage. Note the log scaling of the discharge axis—the rating curves differ by more than 100% for stages above 14 feet. The maximum recorded stage between water years 2013–2020 was 19.8 feet, at which level the rating curves differ by 150%. To demonstrate the stability of the SWE-derived rating model, the jackknife resampled rating curves (Table 2) fit approximately within the thickness of the line.*

*\* Note that in all cases the “SWE-derived” rating curve was created using both SWE measurements and low-stage USGS discharge measurements.*

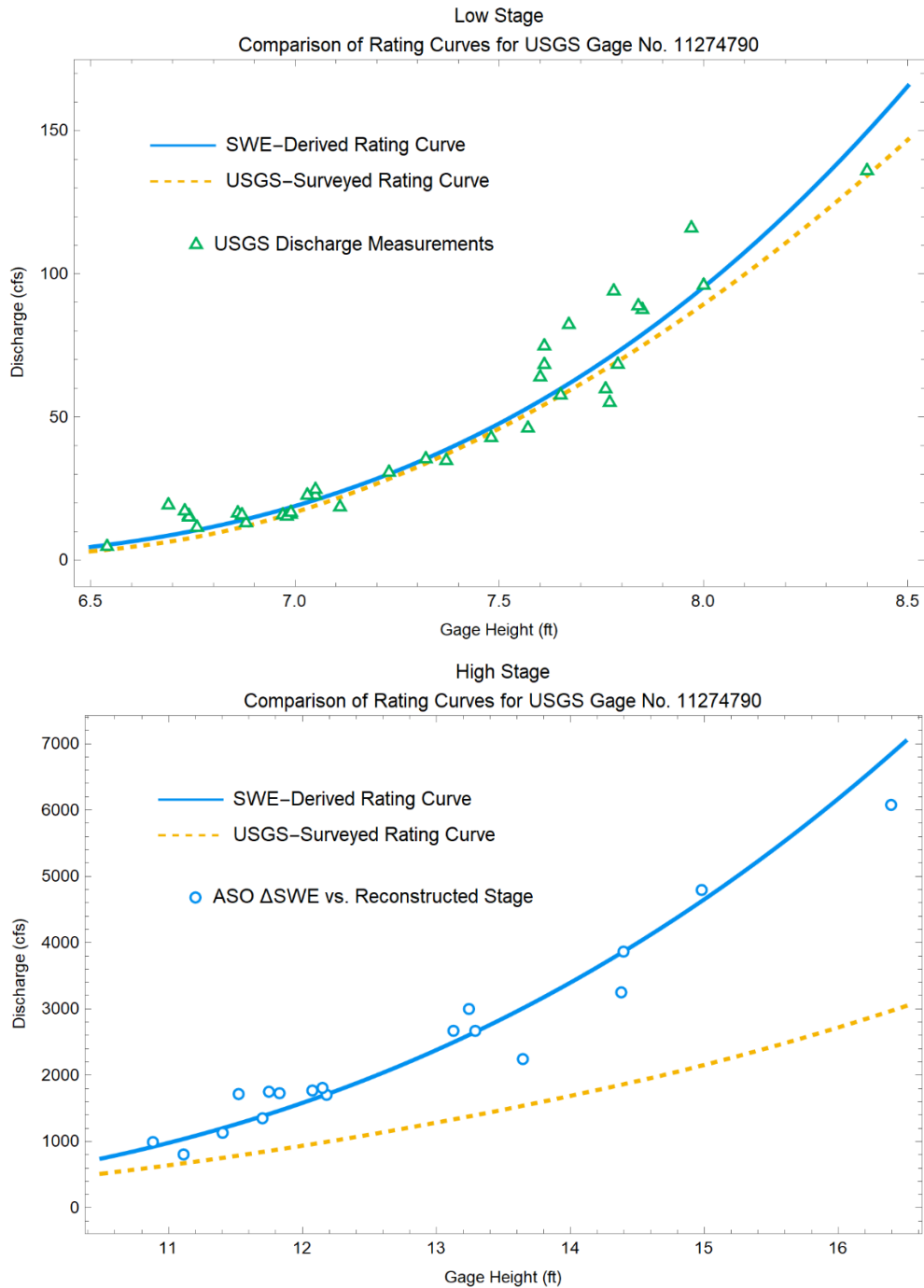


**Figure 4: Comparison of rating curves at low and high stages**

*The panels show sections of the rating curves plotted with linear axes to emphasize agreement or discrepancy. The SWE-derived and USGS-surveyed rating curves are similar in the range of the low-stage USGS discharge measurements (upper panel). The SWE-derived curve indicates high-stage discharge levels roughly twice as large as the surveyed rating curve (lower panel), causing the SWE-derived curve to diverge from the surveyed curve at high stage.*

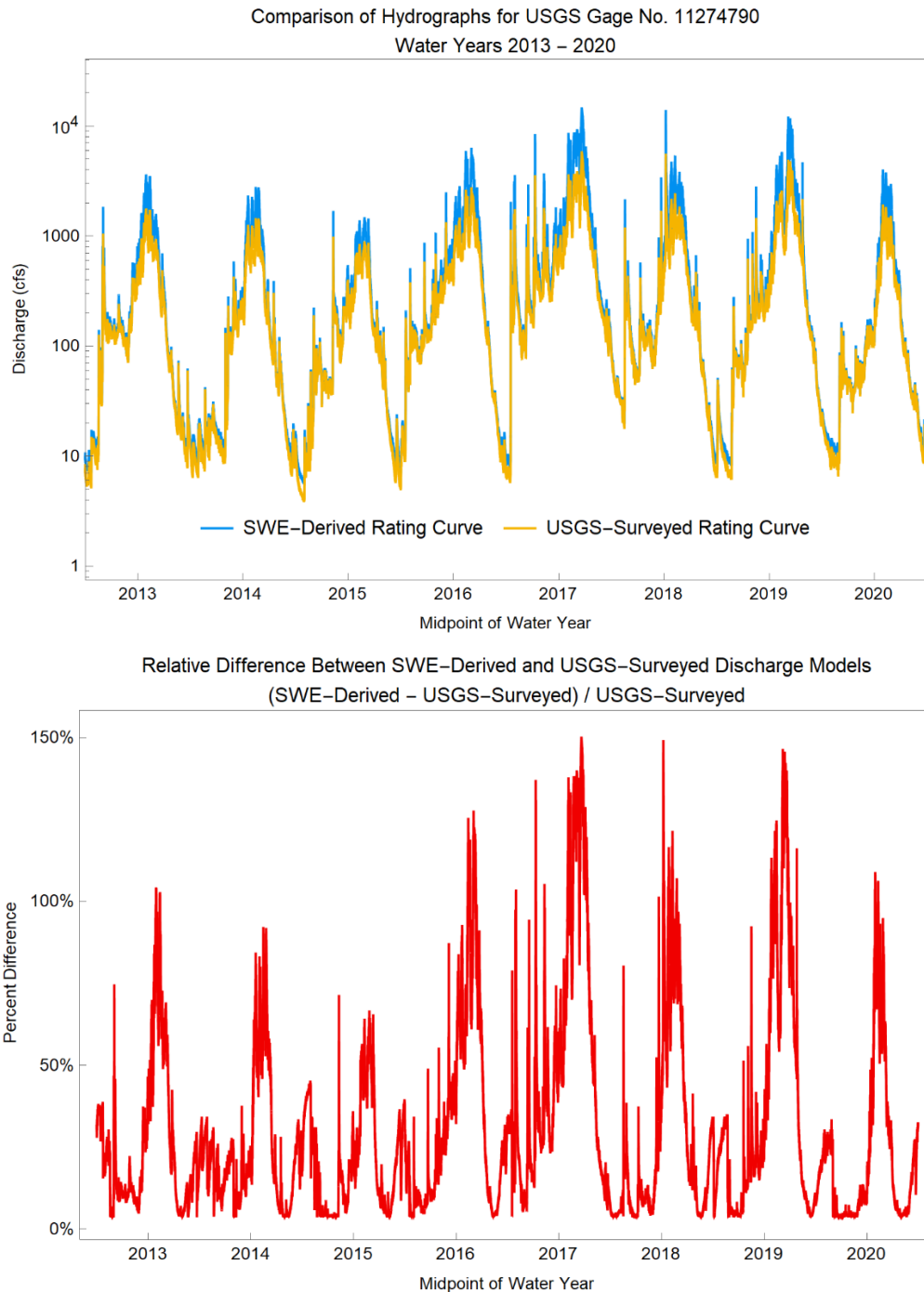


**Figure 5: Comparison of headwaters hydrographs for water years 2013–2020**

*The top panel shows 14-day smoothed hydrographs produced by the proposed new rating curve and the USGS-reported daily discharge values for water years 2013–2020. The bottom panel shows daily percent difference of the modeled discharge versus the original hydrograph. The SWE-fitting approach indicates peak melt-season discharge more than 100% higher than the discharge values reported by the USGS.*

As a further check on the new model, we repeat our methods leading to Figure 2 using the SWE-derived rating curve to calculate 15-minute discharge from the stage record instead of using the USGS-reported discharge. The re-modeled discharge record indicates that the headwaters basin initially underperforms the full basin before “catching up” later in the melt season (Figure 9).

To investigate the seasonal dependence of the relative water balance, we posit a relationship between temperature and snowmelt elevation. We obtain mean monthly freezing elevations (mean 0°C isotherms) by calculating average temperatures at the Hetch Hetchy Meteorological Station (HEM, elevation 1195 m) and the Tuolumne Meadows Meteorological Station (TUM, elevation 2621 m) and reconstructing monthly mean adiabatic lapse rates between these stations (CA Dept. Water Resources 2021). We create hypsometric curves for the full basin and headwaters subbasin to obtain an estimate of the area of each catchment lying below the mean monthly thaw elevation (Painter et al. 2020 DTM). Ratioing these monthly thaw areas gives the relative seasonal variation in unfrozen area between the basins.

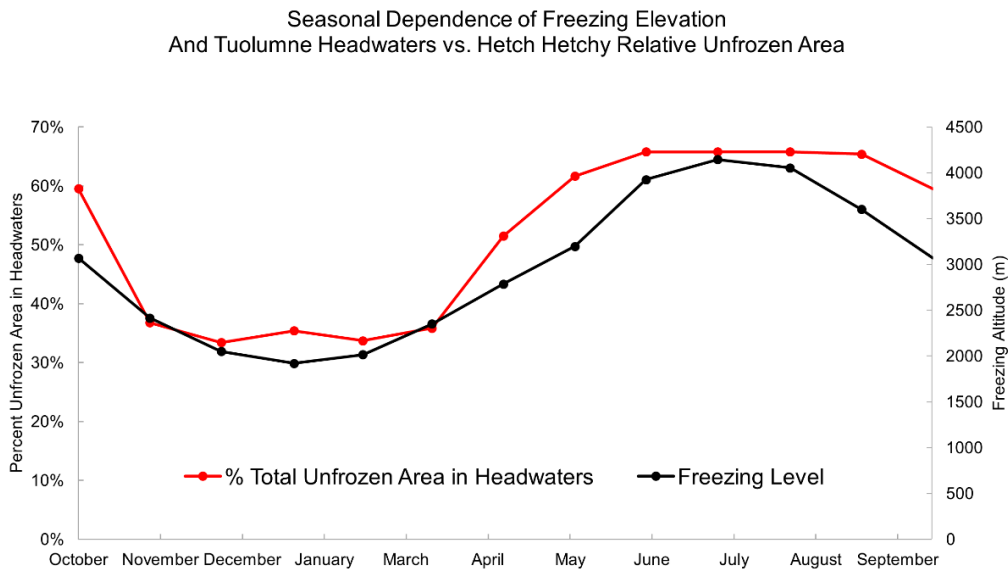


**Figure 6: Freezing elevation versus relative headwaters unfrozen area**

*The freezing elevation is computed from monthly mean temperatures and lapse rates between two meteorological stations in the study region. We use these freezing elevations with a hypsometric curve to derive the relative unfrozen area of the headwaters subbasin compared to the full basin. The headwaters subbasin has relatively little unfrozen area in the early season (around 30-40%), but once the 0°C isotherm moves to high altitudes, the relative unfrozen area converges on the total relative area of 66%.*

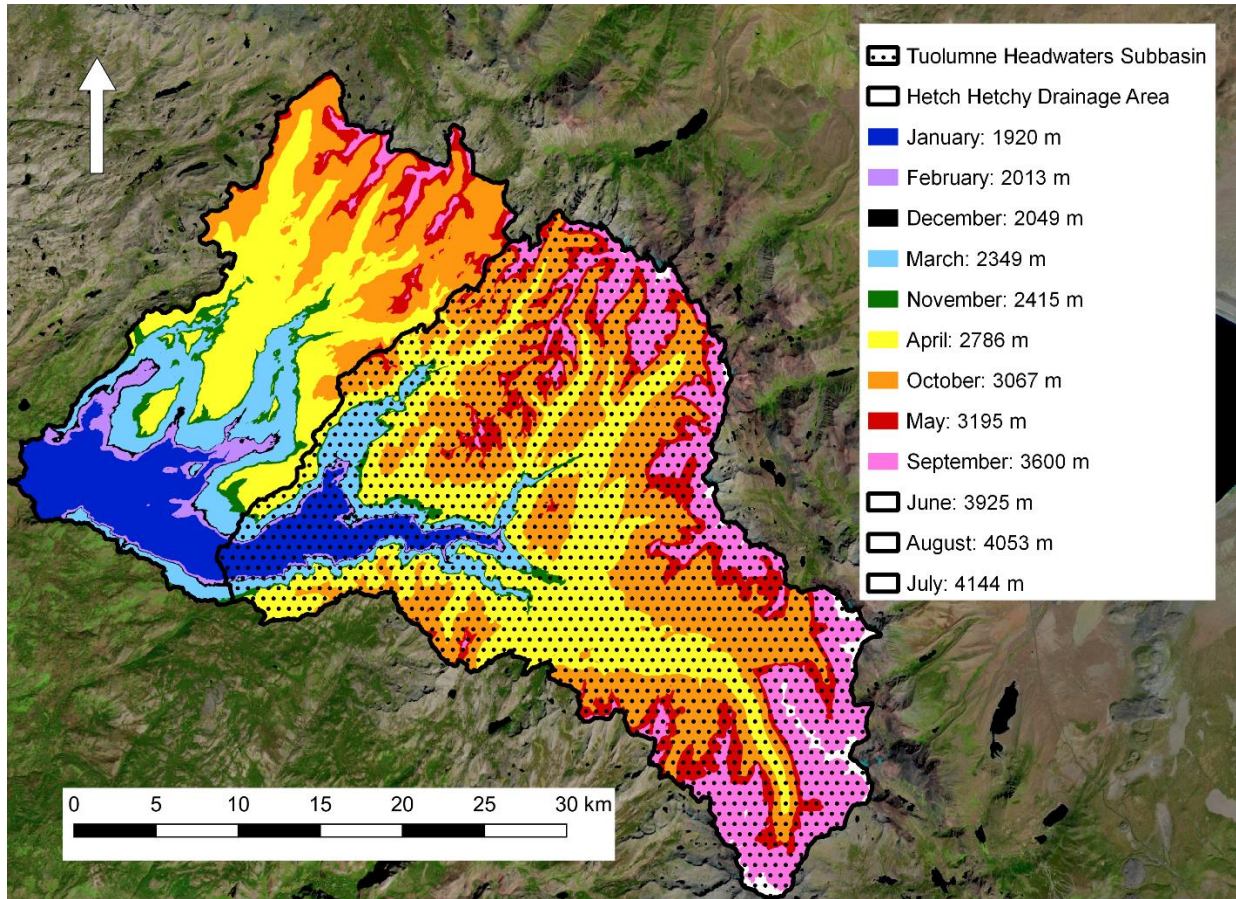


**Figure 7: Mean monthly unfrozen areas**

*The map shows the areas below each monthly mean  $0^{\circ}\text{C}$  isotherm, with the months listed in order from lowest to highest average freezing elevation. Note that the colder months have more relative melted area in the non-headwaters portion of the Hetch Hetchy drainage basin.*

Early in the melt season, the headwaters subbasin includes approximately 35% of the total unfrozen area, but once the  $0^{\circ}\text{C}$  isotherm moves into the alpine regions around May, the headwaters subbasin exceeds 60% of the total unfrozen area. The relative seasonal dependence of unfrozen area on basin hypsometry correlates with the relative discharge trend which we observe from the new SWE-derived rating curve.

To interrogate the processes driving this relationship, we show that the relative SWE melt is correlated with the relative freezing area. For each of the 48 inter-flight SWE measurement periods, we identify all pixels with snow loss, even on intervals with net SWE gain. Binning these pixels into 100 m elevation contour bands, normalizing by the maximum SWE depth loss on each interval, and arranging by day of year reveals that the majority of SWE melt generally

occurs near or below the interpolated mean freezing altitude. Several of the earliest periods are outliers from this trend, but we note that the SWE maps do not account for rain on bare-ground areas; in the early periods, with low snowmelt magnitude, small low-elevation rainstorms precipitating directly into or around the reservoir will likely dominate the input side of the catchment water balance (Boardman et al. 2021, unpublished). In this case, too, our isotherm hypsometry predicts a relatively low headwaters contribution to early season inflow due to the lower relative amount of unfrozen area experiencing liquid precipitation.

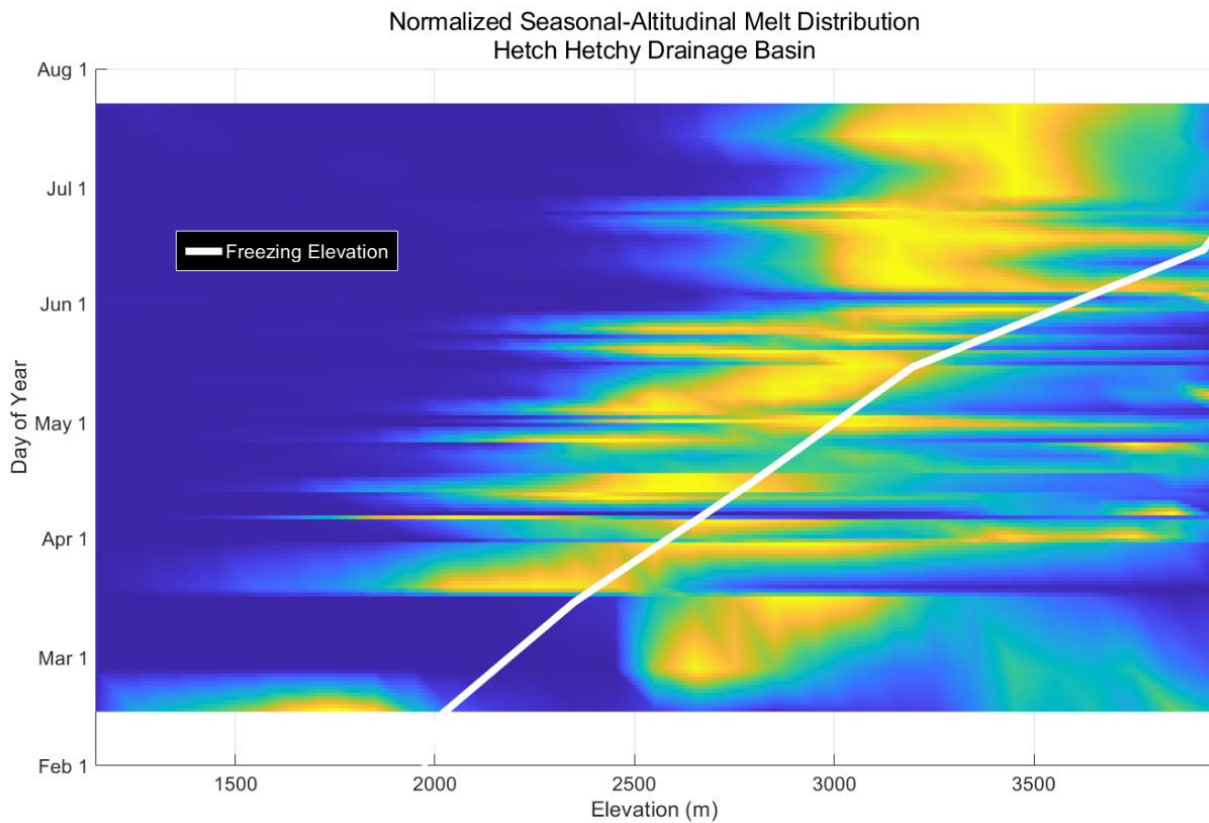


**Figure 8: Seasonal dependence of the dominant SWE loss elevation range**

*The plot shows an interpolated surface representing SWE loss (in period-normalized depth) as a function of elevation (100 m contour band) and day of year. The white line shows the mean monthly 0°C isotherm from Fig. 6, which roughly aligns with the midpoint to upper bound of the primary melt area at any given time.*

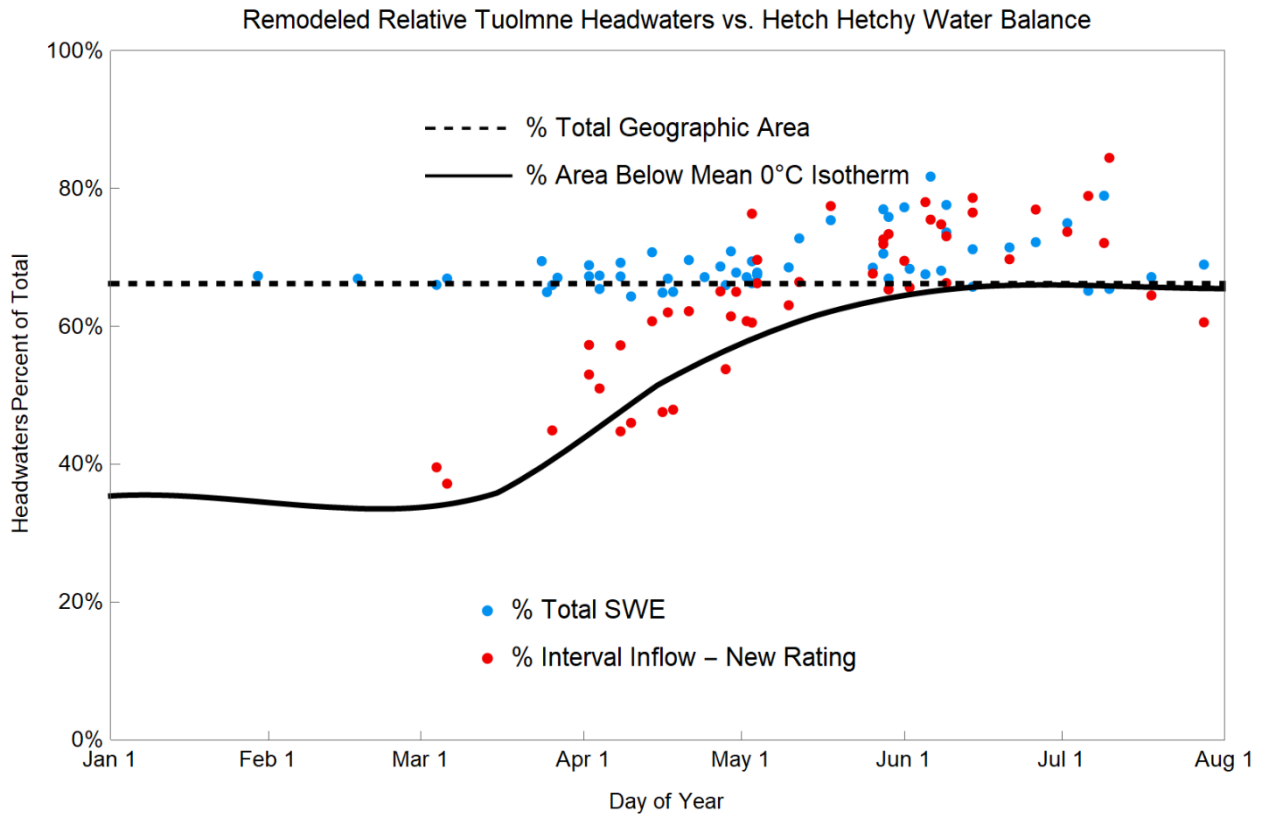


**Figure 9: Re-modeled relative balances of SWE and runoff for the headwaters subbasin**

*The relative SWE content of the headwaters subbasin (blue points) is roughly proportional to its fractional geographic area compared to the full Hetch Hetchy Reservoir drainage area (dashed line). In the later season, the headwaters subbasin includes slightly above-average SWE due to its slightly higher elevation. However, the relative integrated discharge values between each ASO flight (red points) show that the headwaters subbasin produces relatively little water early in the season. The seasonal dependence of relative headwaters runoff aligns with the interpolated relative mean unfrozen area in the subbasin (solid line), which we derive from a freezing elevation isotherm using basin hypsometry. Compare to Fig. 2.*

We conclude that the SWE-derived rating curve correctly captures the seasonal dependence of relative headwaters discharge contributions due to the differential full basin and subbasin hypsometry and the accompanying variation in relative unfrozen areas.

## **Discussion**

We attribute the discrepancy between headwaters basin SWE percentage and relative runoff (Fig. 2) to error in the survey-derived rating curve and propose that our new rating curve, derived from distributed SWE loss measurements and USGS field measurements, should be considered for rating discharge from USGS Gage Number 11274790 since it gives a more reasonable water balance relationship (Fig. 9).

Our water balance analysis for the headwaters subbasin of Tuolumne River demonstrates the sensitivity of measurements of total yearly discharge to errors in the upper end of the rating curve since the majority of the year's water passes the gage in a relatively short snowmelt season. Small errors in hydraulic simulation cause enormous discrepancies in modeled discharge.

By comparing known reservoir inflows and known full-basin SWE changes, we can identify periods of near 1:1 correlation between snowmelt and runoff. Using the local SWE loss rate during these periods as a proxy for headwaters discharge, we obtain proxy high-flow rating data. Estimates of high-stage rating data were previously obtainable only with extensive on-site trolley equipment or dilution materials, both of which are contraindicated in the upper Tuolumne River watershed. Thus, airborne mapping of SWE enables a new approach to calibrating high-discharge rating curves in Wilderness settings.

Our numerically optimized power-law rating model ignores the local reach morphology, yet the model still reduces the mean relative water balance error from 40% to 6% across the melt seasons of 2013–2019. Furthermore, the new model enables interesting comparisons, such as the freezing area versus relative runoff relationship demonstrated in Figs. 6-8.

We suggest that careful use of SWE loss as a proxy for high-stage discharge is a useful technique for fitting rating curves at gaging sites which are difficult to calibrate through traditional means.

## **Acknowledgements**

We acknowledge the contribution of Dr. Thomas Painter, Dr. Jeffery Deems, and Dr. Kat Bormann of Airborne Snow Observatories, Inc., to helping identify the initial water balance discrepancy and providing additional insight on aspects of the project. This acknowledgement does not imply any implicit or explicit endorsement of the methods and results contained herein.

## References

- Boardman, E., Dethier, E., Renshaw, C. (2021, unpublished). Eco-Terrain Zone Importance in Runoff Modeling: Unmixing Components of Basin Efficiency Using Detailed Snowmelt Maps. Dartmouth College Department of Earth Sciences, senior thesis. In progress.
- California Department of Water Resources. Meteorological Station Data, HEM and TUM. Accessed 2021.  
[https://cdec.water.ca.gov/dynamicapp/staMeta?station\\_id=HEM](https://cdec.water.ca.gov/dynamicapp/staMeta?station_id=HEM)  
[https://cdec.water.ca.gov/dynamicapp/staMeta?station\\_id=TUM](https://cdec.water.ca.gov/dynamicapp/staMeta?station_id=TUM)
- Conrad, O., Bechtel, B., Bock, M., Dietrich, H., Fischer, E., Gerlitz, L., Wehberg, J., Wichmann, V., and Bichner, J. (2015): System for Automated Geoscientific Analyses (SAGA) v. 2.1.4, *Geosci. Model Dev.*, 8, 1991-2007, doi:10.5194/gmd-8-1991-2015.
- GDAL/OGR contributors (2021). GDAL/OGR Geospatial Data Abstraction software Library. Open Source Geospatial Foundation. <https://gdal.org>
- Graham, C. (2018). ASO in the Tuolumne River Basin: Forecasting streamflow using basin wide SWE estimates (presentation). Yosemite Hydroclimate Meeting.
- GRASS Development Team, (2017). Geographic Resources Analysis Support System (GRASS) Software, Version 7.2. Open Source Geospatial Foundation. Electronic document.: <http://grass.osgeo.org>
- Hedrick, Andrew R., Danny Marks, Scott Havens, Mark Robertson, Micah Johnson, Micah Sandusky, Hans-Peter Marshall, Patrick R. Kormos, Kat J. Bormann, and Thomas H. Painter. "Direct Insertion of NASA Airborne Snow Observatory-Derived Snow Depth Time Series Into the ISnobar Energy Balance Snow Model." *Water Resources Research* 54, no. 10 (2018): 8045–63. <https://doi.org/10.1029/2018wr023190>.
- Henn, B., Painter, T. H., Bormann, K. J., McGurk, B., Flint, A. L., Flint, L. E., White, V., Lundquist, J. D. (2018). High-elevation evapotranspiration estimates during drought: Using streamflow and NASA airborne snow observatory SWE observations to close the upper tuolumne river basin water balance. *Water Resources Research*, 54,746–766. <https://doi.org/10.1002/2017WR020473>
- MATLAB. (2020). *R2020a*. Natick, Massachusetts: The MathWorks Inc.
- McGurk, B. (2021). General Discussion. Personal communication.
- McGurk, B. (2021). Hetch Hetchy Reservoir Inflows. Personal communication.

- Painter, T., Berisford, D., Boardman, J., Bormann, K., Deems, J., Gehrke, F., Hedrick, A., Joyce, M., Laidlaw, R., Marks, D., Mattmann, C., Mcgurk, B., Ramirez, P., Richardson, M., Skiles, S.M., Seidel, F., and A. Winstral (2016): The Airborne Snow Observatory: fusion of scanning lidar, imaging spectrometer, and physically-based modeling for mapping snow water equivalent and snow albedo. *Remote Sensing of Environment*. DOI: 10.1016/j.rse.2016.06.018
- Painter, T., et al. (2019). ASO L4 Lidar Snow Water Equivalent 50m UTM Grid, Version 1. Tuolumne Basin. Boulder, Colorado USA. NASA National Snow and Ice Data Center Distributed Active Archive Center. doi: <https://doi.org/10.5067/M4TUH28NHL4Z>. Accessed 2021.
- Painter, T. H., K. J. Bormann, et al. (2020). *ASO L4 Lidar Point Cloud Digital Terrain Model 3m UTM Grid, Version 1*. Tuolumne Basin. Boulder, Colorado USA. NASA National Snow and Ice Data Center Distributed Active Archive Center. doi: <https://doi.org/10.5067/2EHMWG4IT76O>. Accessed 2021
- QGIS.org (2021). QGIS Geographic Information System. QGIS Association. <http://www.qgis.org>
- Rantz, S.E. (1982). Measurement and computation of streamflow. U.S. Geological Survey Water-Supply Paper 2175, p. 631. Reston, Virginia.
- U.S. Geological Survey (2021). Stage Data, Field Measurement Data, and Rating Curve for Gage Number 11274790. Accessed 2021. [https://waterdata.usgs.gov/nwis/inventory/?site\\_no=11274790&agency\\_cd=USGS](https://waterdata.usgs.gov/nwis/inventory/?site_no=11274790&agency_cd=USGS), [https://waterdata.usgs.gov/nwis/inventory/?site\\_no=11275500&agency\\_cd=USGS](https://waterdata.usgs.gov/nwis/inventory/?site_no=11275500&agency_cd=USGS).
- Wolfram Research, Inc., (2020). Mathematica, Version 12.2, Champaign, IL.